

THE CORONA MASS FLOW METER

Fredrik Laurantzon^{*}, Nils Tillmark[†] and P. Henrik Alfredsson[‡]
KTH CICERO, Dept. Mechanics, Royal Institute of Technology,
SE-100 44 Stockholm, Sweden

ABSTRACT

In many turbo machinery applications it is of interest to be able to measure the mass flow of the gas. However, to measure mass flow accurately is complicated and especially to obtain time resolved mass flow measurements. In the present research we are developing and testing a mass flow meter based on the transport and interaction of ions with a flow field. The ions are generated through a corona discharge, by applying a high electric potential to a thin wire which is mounted in the flow field. The positive ions thereby created, are attracted to two separated wall electrodes. The ions will deflect in different ways to the wall electrodes depending on the flow rate normal to the electric field. As a consequence, the electrical current to the wall electrodes differ and the difference is proportional to the mass flow rate. Preliminary results show that there is a linear relation between the difference current and the mass flow rate, and that it is fairly insensitive to the flow profile.

INTRODUCTION

For turbo charged internal combustion engines it is important to know the mass flow in various branches of the gas exchange system in order to be able to accurately control and tune the engine for best performance. However the flow situation is usually non-ideal, with complex highly three-dimensional pipe geometries, pulsating flow, reversed flow, temperature and pressure variations as well as particulates (soot etc.). These complications make standard techniques (such as hot-film) less suitable. One method which has been suggested (see refs. [1],[2],[3]) is based on transport of ions created by a corona discharge in the flow, in the following we will denote this the Corona mass flow meter (CMFM).

Potential benefits with the Corona mass flow meter compared to other flow measurement methods are that it has

a potential to achieve a rapid response and that it can handle reversed flows. Furthermore it seems to be fairly insensitive to the inlet profile and one may assume that the measurement averages the mass flow rate across the cross section.

In the present paper we demonstrate some preliminary results for a corona flow meter set-up and discuss some planned future developments and tests of the method.

BACKGROUND TO THE CORONA MASS FLOW METER

When a high voltage is applied to a metallic object with a small radius of curvature and there is a grounded metallic surface at some distance from it, a corona is formed in a region around that object. The object could be point wise (like a needle tip) or of cylinder type (i.e. a thin wire). In the following we will discuss the latter which is used widely in various technical applications such as photocopiers and electrostatic precipitators.

The geometry used for the present corona mass flow meter is a coaxial arrangement with two outer grounded metallic cylinders (cathodes) and an inner thin metal wire (anode) with radius a . When applying a high (positive) direct current voltage to the wire, natural free electrons are accelerated towards the wire and at high enough speeds collisions between electrons and gas molecules give rise to ionized molecules (in air mainly O_2^+ and N_2^+) and new electrons. In the coaxial arrangement the electric field strength is

$$E(r) = E_w \frac{a}{r}$$

where r is the radius from the centre of the wire and E_w is the field strength at the wire surface. The electric field strength at a smooth surface wire when a corona is formed is given by the empirical expression

$$E_{w,corona} = 3 \cdot 10^6 (1 + 0.03a^{-1/2}) \text{V/m}$$

known as Peek's formula where a should be given in meters.

^{*}laurantzon@mech.kth.se, [†]nt@mech.kth.se, [‡]hal@mech.kth.se

The corona region is usually assumed to exist where the electric field strength is larger than $3 \cdot 10^6$ V/m and for a wire with a radius of $a=25 \mu\text{m}$ the corona region would hence reach out to $r \approx 7a$. The physical reason for the existence of such a boundary is that ionization and attachment of electrons balance at this radius.

It is also possible to estimate the voltage potential at the wire which is needed in order to establish the corona. For a wire with a radius of $25 \mu\text{m}$ and with the distance to the cathode of 24 mm the voltage needed is estimated to about 3.6 kV.

The geometry of a corona mass flow meter may vary, however in the present set-up the co-axial arrangement using a thin wire to which a high positive voltage is applied for the corona discharge is utilized. The wire is mounted concentrically with two identical outer hollow cylindrical electrodes which are located along the inner pipe wall. The electrodes are axially separated by a couple of millimetres (see Fig. 1). When the potential of the wire is sufficiently large, the gas around and close to the thin centre wire will ionize and positive ions are attracted to the two wall electrodes. When gas is flowing through the mass flow meter, the number of ions which reaches the downstream electrode will be larger than for the upstream electrode, thereby making $i_2 > i_1$. Each wall electrode is connected to a precision resistor which both have the same resistance R . The voltage potential difference ($\Delta V = V_2 - V_1$) between the top of both resistors is then related to the difference in currents ($\Delta i = i_2 - i_1$) through the two wall electrodes as $\Delta i = \Delta V/R$. It is obvious from the above description and from Fig. 1 that if the flow is reversed then also the output will change

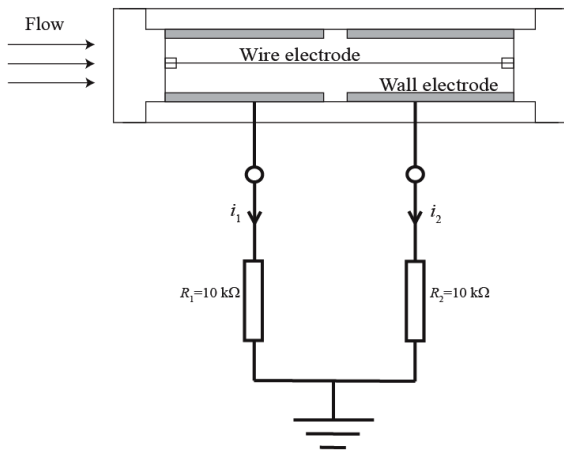


Fig. 1 Principle of the corona mass flow meter.

sign.

The output from the CMFM depends on several geometrical and physical parameters. Obviously the voltage applied to the the corona wire has to be high enough for the corona to form and if the corona is formed the current density will increase with increasing voltage potential at the wire. The wire diameter $2a$ is a crucial parameter and the smaller the diameter the smaller the applied voltage can be in order to establish a corona. Also the diameter ($2R$) of the pipe and hence the distance from the wire to the wall cathode will influence the current through the gas. For the frequency response of the CMFM the length (L) of the cathodes and their axial separation (Δ) may be important or rather the non-dimensional parameters L/R and Δ/L .

EXPERIMENTAL SET UPS

The corona mass flow meter used in the present study has a pipe diameter ($2R$) of 48 mm and the diameter ($2a$) of the corona wire is $50 \mu\text{m}$. The corona wire is made from stainless steel and mounted in the centre of the pipe supported by two Plexiglas supports. The voltage is provided at the upstream end of the wire. The wall electrodes are made of brass with a thickness of 1 mm and both have a length of $L=90$ mm and are separated by $\Delta=10$ mm. The wire voltage was provided by a high voltage DC power supply and for the present configuration an electrical current was obtained for voltages above approximately 7 kV. This value is about twice as high as predicted by the theory described above. The maximum tested voltage was 16 kV.

Two experimental flow set-ups have been used to evaluate the CMFM described above. The first set-up (see Fig. 2a) consisted of a straight pipe where the air flow is drawn through a nozzle connected to the CMFM through constant area piping. Downstream of the CMFM a variable rpm fan is connected through which the flow rate can be set. With the fan used the maximum mass flow rate was 56 g/s corresponding to a mean velocity in the CMFM of 26 m/s. The flow rate was determined by measuring the pressure difference over the inlet nozzle.

The second set-up (see Fig. 2b) was used in order to study the frequency response of the CMFM. Downstream of the inlet a rotating disc valve with its shaft connected to a DC motor periodically obstructs the flow giving a pulsating flow in the pipe. The flow rate can be approximately determined with an LDV system. The measurement volume can be traversed across the pipe and the flow rate integrated in a phase averaged sense (i.e. as function of the valve opening position). The flow

is seeded with small droplets and the big chamber after the bend is a filter removing the droplets before the air enters the CMFM.

The LDV-system consists of a 4W Ar-ion laser, fiber optics probe head with 500 mm focal length and a beam intersection angle of 6.8° . The intersection volume has a diameter of 0.3 mm. The measurement section consists of a 200 mm long glass pipe with an inner and outer diameter of 60 and 65 mm respectively, located just downstream the rotating disc. The traversing system used is from ISEL and the measuring volume can be traversed in three orthogonal directions. The velocity was measured in three points at a cross section normal to the pipe axis: one at the centreline ($r/R = 0$) and the two other at the half radius away from the centre ($r/R = \pm 0.5$).

The LDV processor and software is from Dantec Dynamics. The seeding generator is of nebulization type injecting small droplets upstream the rotating disc. A tachometer connected to the rotating shaft gives an input signal to the LDV processor once each revolution. In this fashion, the time/phase of the velocity measurements is reset at a certain angle of the rotating disc. The sample rate is about 100 Hz and the measurement time

approximately 5 minutes at each position, which gives reliable data to evaluate the velocity during a cycle.

RESULTS

Steady state measurements

Fig. 3 shows typical calibration curves for different corona voltages. As can be seen the sensitivity of the CMFM increases with increasing applied wire voltage. It is also clearly observed that the linearity of the output becomes better with higher voltage applied to the corona wire. There is an almost linear relationship between the current difference (Δi) and the mass flow rate at the highest corona voltage which is 16 kV in this case.

The current difference at no flow is not zero and increases with increasing wire voltage. This can be inferred to be an effect of a slight geometrical difference between the two electrodes and has no practical implications because it can easily be taken care of during the calibration. The current difference is quite small, but can still be detected with good accuracy. With precision resistors of 10 k Ω the voltage measured at $\Delta i = 1 \mu A$ is 10 mV which is resolvable with high accuracy without any problems either with a digital voltmeter or an AD-converter for acquisition through a computer. A typical electrode current is 10 μA at a corona voltage of 16 kV.

Fig. 4 shows three different calibration curves. Two of them show measurements with a straight inlet which are taken with a 90 minutes time difference. This shows that repeatability of the calibration is good. The third curve shows the calibration when the straight inlet flow has been exchanged with a curved pipe flow inlet, thereby giving a highly skewed inlet flow profile. As can be seen

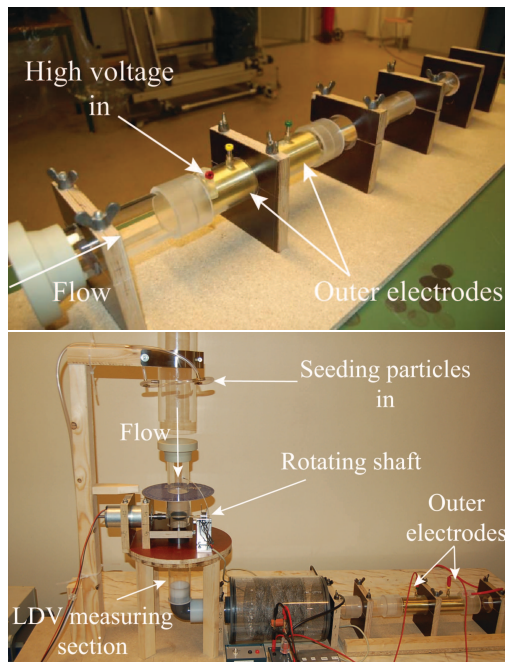


Fig. 2 a) Flow set-up number 1 for calibration purposes, b) flow set up 2 which allows for accurate dynamic calibration.

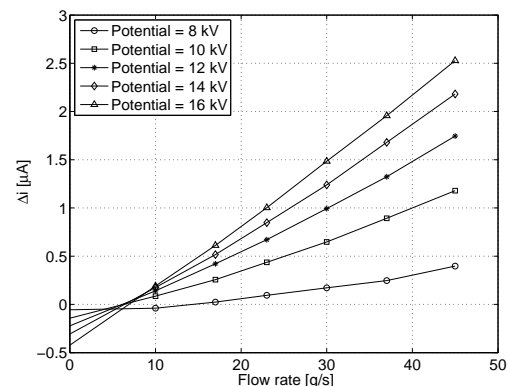


Fig. 3 Calibration curves for different applied potentials.

the calibration curve seems to be insensitive to the profile shape.

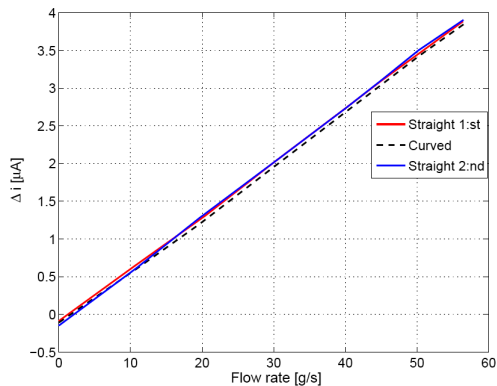


Fig. 4 Calibration curves for different inlet flow profiles at 16 kV.

Dynamic measurements

The frequency response of the CMFM was tested for two different frequencies of the rotating valve, namely 1.5 Hz and 15 Hz giving twice the frequency of the pulses in the flow.

Results from the LDV measurement can be seen in Fig. 5, where the velocity at the centreline ($r = 0$) and at $r = \pm R/2$ of the measuring position depicted in Fig. 2b, is shown as function of the phase. This figure is the result of an averaging over about 5 min. The shaft frequency was 15 Hz in all three cases, which implies pulses at 30 Hz. The mean velocity at the same conditions but with the valve fully open was 12.5 m/s. As can be seen the two pulses are not exactly the same on both sides of the pipe and the peaks are slightly higher away from the centre. It can be noted that the velocity does not go to zero at the point where the valve is closed. The average velocity of the three positions are 7.4, 7.2 and 9.2 m/s. If these values are used to get an average velocity (i.e. 7.9 m/s) the mass flow rate becomes 26.9 g/s.

In Fig. 6 the mass flow rate measured by the corona meter, is plotted versus time for the frequencies 3 and 30 Hz respectively. In the 3 Hz case the pulses are regular whereas in the 30 Hz case there is a fairly large variation. However what is clearly evident is that in neither case does the mass flow rate go down to the flow rate indicated by the LDV measurements. This is especially pronounced for the high frequency case. However the mean flow (for the 30 Hz case) is almost the same as determined from the LDV measurements (27.5 g/s and 26.9 g/s, respectively).

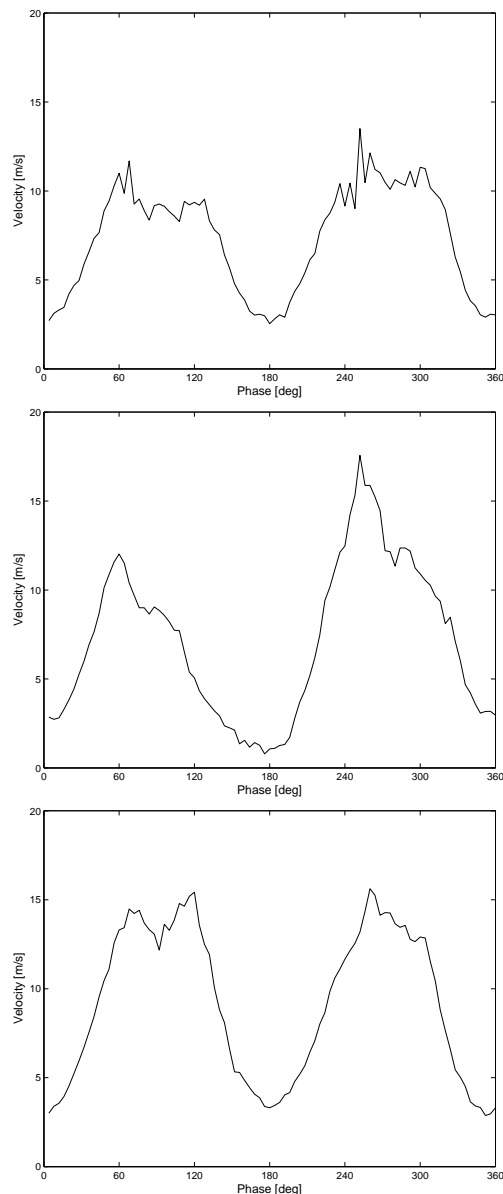


Fig. 5 Phase averaged velocity at $r = 0$ and $r = \pm R/2$, obtained from LDV measurements.

In Fig. 7 the phase averaged (over 10 realizations) mass flow measurements are shown. Although the averaging takes away a large part of the scatter the difference compared to the LDV is even clearer. Two reasons for the apparently bad frequency response seem feasible. The first would be to assume that the frequency response of the CMFM itself is low. However one may estimate, that with the present flow rate the velocity should be around

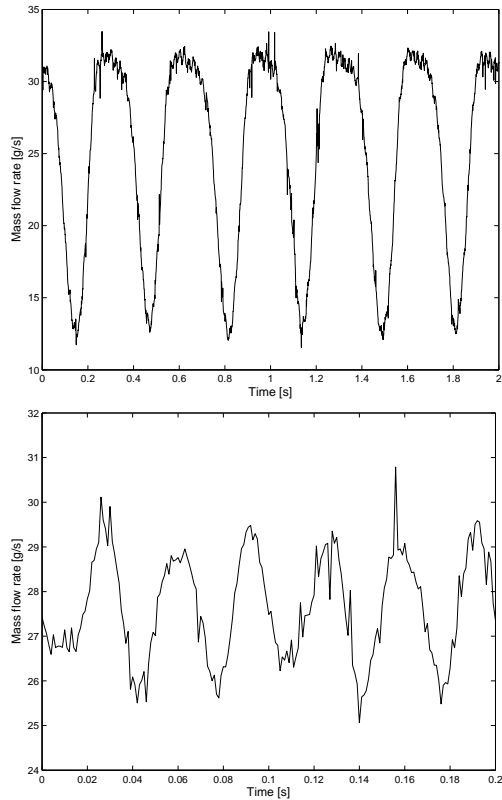


Fig. 6 Pulsating flow signals from the CMFM at 3 Hz (upper) and 30 Hz (lower). The mean mass flow rate is 25.2 g/s and 27.5 g/s, respectively.

13 m/s in the test section and at a frequency of 3 Hz the pulse length should correspond to 4 m, which should clearly be resolvable by the present geometry. The second possibility is that the flow at the position of the CMFM is not the same as measured by the LDV and that the pulses are smeared out along the pipe and especially in the filter filled cavity.

CONCLUSIONS

Steady state tests shows that the CMFM has good accuracy and the desired linearity if the wire voltage is high enough. The response of the CMFM was found to be insensitive to the flow profile. However further tests to try out its steady state performance are planned. Several parameters such as gas temperature, gas pressure, level of humidity may affect the response. Also the sensitivity to particles and other contaminants is of interest.

The tests for the frequency response described here are so far inconclusive. In the present work the flow rate

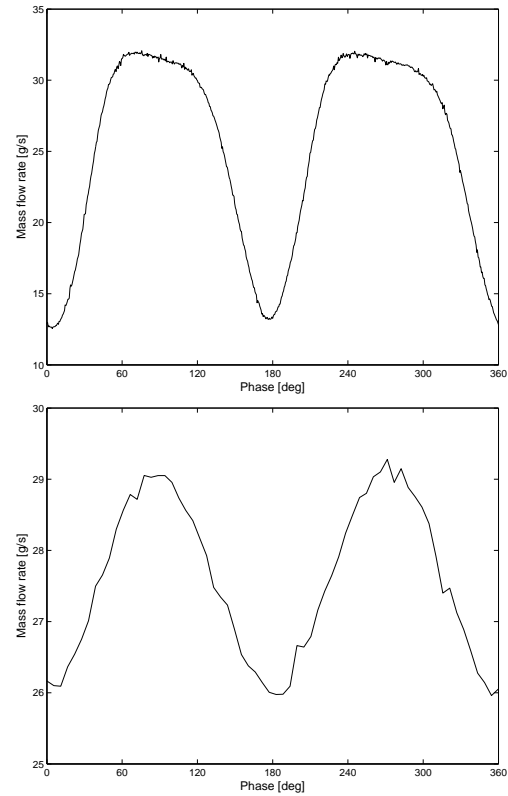


Fig. 7 Phase averaged output signal from the CMFM at 3 Hz (upper) and 30 Hz (lower) (same data as in Fig. 6).

was determined by the LDV at some distance from the installation of the CMFM, however it need to be measured close to the installation in order to draw any firm conclusions. However the response can certainly be improved by decreasing the length of the anode and the cathodes, although as always this will also decrease the sensitivity of the measurement system. In order to determine the influence of various geometrical parameters we plan to do numerical modelling of the CMFM in the future.

ACKNOWLEDGEMENTS

This work was supported by CICERO (Centre for Internal Combustion Engine Research Opus), a competence centre at KTH, sponsored by the Swedish Energy Agency, vehicle industry in Sweden and KTH.

REFERENCES

- [1] Balachandran, W., Machowski, W. & Horner, W. 1999 Electrostatic mass air flow meter. Institute of Physics Conference Series 163, 269-274.
- [2] Malczynski, G.W. & Schroeder, T. 1992 An ion-drag air mass-flow sensor for automotive applications. IEEE Transactions on Industry Applications 28, 304309
- [3] Tanaka, M., Kitajima, U., Fujibayashi, K., Doi, S. & Sato, T. 1989 A study of corona discharge air mass flowmeter. The Japan Society of Mechanical Engineers, No. 88-1011 A. pp. 2533-2539.
- [4] Chen, J. & Davidson, J.H. 2002 Electron density and energy distributions in the positive DC corona: Interpretation for corona-enhanced chemical reactions. Plasma Chemistry and Plasma Processing. **22**, 199-224.